Demonstration of Environmentally Stable, Broadband Energy Dissipation via Multiple Metal Cross#Linked Glycerol Gels

Citation: Cazzell, S. A., Duncan, B., Kingsborough, R., Holten-Andersen, N., Demonstration of Environmentally Stable, Broadband Energy Dissipation via Multiple Metal Cross-Linked Glycerol Gels. Adv. Funct. Mater. 2021, 31, 2009118

As Published: http://dx.doi.org/10.1002/adfm.202009118

Publisher: Wiley

Persistent URL: https://hdl.handle.net/1721.1/140287

Version: Author's final manuscript: final author's manuscript post peer review, without publisher's formatting or copy editing

Demonstration of environmentally stable, broadband energy dissipation via multiple metal cross-linked glycerol gels

Seth Allen Cazzell, Bradley Duncan, Richard Kingsborough, and Niels Holten-Andersen *

Department of Materials Science and Engineering, Massachusetts Institute of Technology, Cambridge, Massachusetts 02139, United States

Lincoln Laboratory, Massachusetts Institute of Technology, Lexington, Massachusetts 02421, United States

E-mail: holten@mit.edu

Abstract

Rapid damping of interfaces experiencing vibrations is critical to the performance of many complex mechanical systems ranging from airplanes to human bodies. Current synthetic materials utilized in vibration damping are limited by either their damping frequency range, tunability, or environmental stability. Here, we demonstrate how single metal ion cross-linked hydrogels exhibit tunable damping across a large frequency range and multiple metal ion hydrogels exhibit broadband damping within a single material. Additionally, we show an enhanced resistance to freezing and dehydration with the use of glycerol as a cosolvent. We expect the material design principles presented here will help advance the development of programmable damping materials better able to meet the demands of sustained operation

This is the author manuscript accepted for publication and has undergone full peer review but has not been through the copyediting, typesetting, pagination and proofreading process, which may lead to differences between this version and the Version of Record. Please cite this article as doi: 10.1002/adfm.202009118

under broad environmental conditions.

Introduction

The performance lifetime of mechanical devices is oftentimes limited by their ability to isolate and protect critical components from absorbing stray energy.[1] The same holds true in nature, where for example the aquatic mussel has faced evolutionary pressure to develop holdfast materials that can successfully withstand repeated mechanical agitation from waves and currents.[2–7] Inspired by these holdfast threads secreted by mussels, molecular engineers have begun to incorporate non-permanent (transient) metal ion cross-links into hydrogels.[8–10] This bio-inspired approach to hydrogel engineering has proven to offer remarkable control over the transient cross-link lifetime via pH, thereby allowing for tunable timescales of damping by the resulting hydrogel. Additionally, it has been shown that the timescale of network damping can be controlled orthogonally from pH through the use of different metal ions in single metal ion gels, and that combining two different metal ions into a dual metal-ion gel can result in a hydrogel network with two distinct timescales of energy dissipation.[9,11,12]

Here, we further the study of using metal ion cross-linked hydrogels as tunable damping materials by cataloging damping as a function of pH in Ni^{2+}, Co^{2+}, Cu^{2+}, and Zn^{2+} single ion gels, as well as in gels containing a combined mixture of these ions. This study thereby uncovers the damping tunability of each metal ion and demonstrates that incorporating complex metal ion mixtures into a single gel can vastly expand the range of damping frequencies. Although this demonstration already represents a promising step towards potential applications in damping, the utility of these hydrogel materials is ultimately limited by their propensity to rapidly dehydrate, whereby the control over timescales of damping is lost.[13] To combat this shortcoming, we describe how the use of glycerol as a cosolvent in metal ion cross-linked hydrogels allows their programmable damping behavior to be maintained while suppressing dehydration. Additionally, we show how the incorporation of glycerol acts to

depress gel freezing, further expanding environmental stability and ultimate utility.

Results and Discussion

Mussel inspired metal-coordinating hydrogels typically consist of hydrophilic poly (ethylene glycol), or PEG, star polymers end-functionalized with a catechol or histidine ligand.[8,9] Here we used histidine as our metal-coordinating ligand instead of catechol for several reasons. First, histidine has a lower pK_a which allows cross-linking to occur under less extreme pH values.[8,9] Second, by using histidine we avoid the covalent cross-linking that can occur between catechol groups, allowing us to focus on the mechanical role played by the metal in controlling the dynamics of a transient bond.[9,14] Third, the coordinate complex binding dynamics of histidine to a range of divalent, first row transition metals such as Ni^{2+}, Co^{2+}, Cu^{2+}, and Zn^{2+} has been well characterized.[9] Previously, histidine hydrogels containing two different metal ions in the same hydrogel have been studied, which is a principle we advance in this study by cross-linking 4-arm histidine star polymers with Ni^{2+}, Co^{2+}, Cu^{2+}, and Zn^{2+} ions within a single hydrogel to create a broadband damping material as shown schematically in Fig. 1 *A*–*C*.[12]

We first examined the tunability of damping via pH within the single ion gels. Traditionally, these single ion metal-coordinate cross-linked hydrogels have been shown, and assumed, to behave like ideal single Maxwell element model materials with a network relaxation time dictated by the metal ion identity and the gel pH.[12] To illustrate this point, we consider two hypothetical single metal ion gels in Fig. 1*D*. Based on an ideal single Maxwell element model (see Materials and Methods section for mathematical description), the different hypothetical metal ions in these single metal materials result in distinct cross-link lifetimes (the inverse frequency of where the polymer network storage and loss moduli are equal) and thereby different timescales of network relaxation at a fixed pH, as illustrated in Fig. 1*E*.[9,11] The ratio of the loss modulus over the storage modulus, the loss factor, or tan , represents

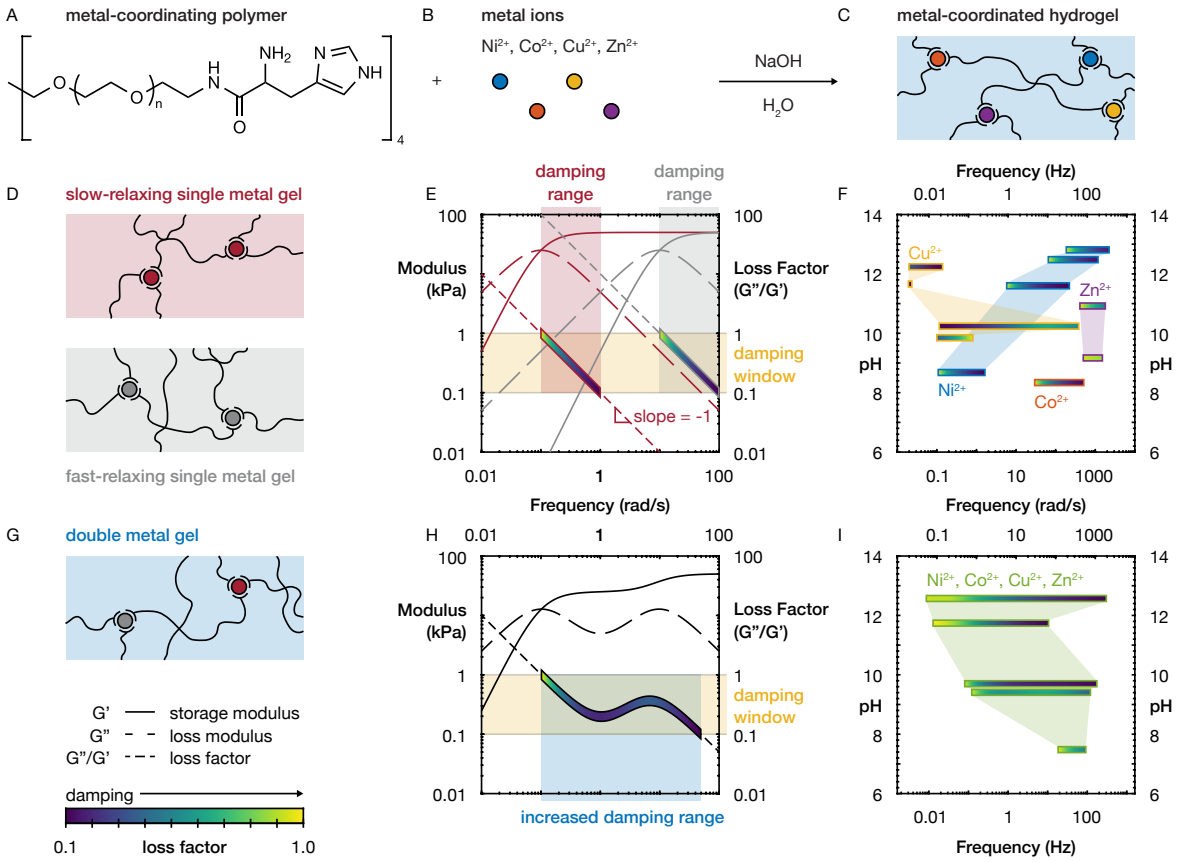

Figure 1: Expanding the damping range in metal ion cross-linked hydrogels. (*A*) Histidine functionalized, 4-arm, 10 kDa poly (ethylene glycol) metal-coordinating polymers can (*B*) bind with multiple first row transition metals such as Ni^{2+}, Co^{2+}, Cu^{2+}, and Zn^{2+} in a single gel to form (*C*) a multiple metal ion coordinated hydrogel. (*D*) Schematic illustrating how separate gels, each formed with a different single metal ion cross-link (one slow-relaxing and one fast-relaxing), results in (*E*) individual theoretical gels (see Hypothetical Frequency Sweeps section of the Materials and Methods) with a single relaxation timescale, dictated by the metal ion identity, which only allows for damping within the target damping window over a relatively narrow frequency range. (*F*) Experimental determination of target damping frequency range in single metal ion hydrogels as a function of pH demonstrates tunable, but narrow, target damping ranges. The shaded regions are interpolations between data sets of single metal ion hydrogels collected at different pH meant as guides to the eye. (*G*) Schematic illustrating how a hydrogel formed with two metal ions leads to (*H*) multiple relaxation timescales in a single theoretical gel, thereby increasing the frequency range of damping within the target damping window. (*I*) Experimental determination of target damping frequency range in hydrogels containing Ni^{2+}, Co^{2+}, Cu^{2+}, and Zn^{2+} as a function of pH demonstrates expanded target damping ranges relative to the single ion hydrogels. The shaded regions are interpolations between data sets of hydrogels collected at different pH meant as guides to the eye.

the degree of mechanical damping, and for these ideal single Maxwell element materials, the loss factor is a straight line with a slope of negative 1, as shown in Fig. 1*E*. For many damping applications it is critical that a material maintains its solid-like characteristics as well, for example to maintain shape. Therefore, a target material damping window of loss factor values between 0.1 and 1 was chosen, with values closer to 1 representing materials that display the most damping while retaining their shape. For the hypothetical single metal ion hydrogels shown in Fig. 1*D*, we can overlay the loss factor within this target damping window with a color bar that indicates the degree of damping, as shown in Fig. 1*E*. For these hypothetical single metal ion hydrogels, the predicted range of mechanical frequencies that match the target damping window are distinct, and relatively narrow.

We performed frequency sweeps on Ni^{2+}, Co^{2+}, Cu^{2+}, and Zn^{2+} single ion hydrogels as a function of pH, to test the prediction of distinct and narrow damping ranges of single metal ion gels. The measured storage and loss moduli are presented in Fig. S1, with the resulting loss factors presented in Fig. S2 *A*–*D*. Only Ni^{2+} ion hydrogels behave as expected, i.e. with a single Maxwell element frequency response tunable with pH, which means that only Ni^{2+} ion gels display a tunable damping frequency range as predicted. This behavior is clearly shown in Fig. 1*F*, where the damping range, and corresponding color bar representing the value of the loss factor between 0.1 and 1, is plotted vs. pH. This plot illustrates that a Ni^{2+} ion hydrogel can be engineered to dampen a narrow range of vibrations predictably by changing the pH. While Zn^{2+} ion hydrogels also display an ideal single Maxwell element frequency response, the gels relax on such short timescales that the target damping window is only matched at high frequencies of oscillations. The gels furthermore only assemble under a narrow pH range, therefore overall showing little tunability. Hydrogels with Co^{2+} ions quickly transition into a permanent, very slowly relaxing, network solid as pH is increased, similar to what has been observed elsewhere when in the presence of a free radical initiator.[15] This permanent increase in the storage modulus at the expense of the loss modulus results in the gel quickly becoming too solid-like to offer anything but a narrow damping range under

limited pH conditions, as shown in Fig. 1*F*. The hydrogels with Cu^{2+} ion behaved somewhat similarly to Co^{2+} ion hydrogels in that they develop a very stable, slowly relaxing material as the pH increases. However, due to their slightly less solid-like behavior, the gel loss factor does enter into the target damping window for each pH tested. Nevertheless, Cu^{2+} ion gel damping behavior is not predictably tunable like Ni^{2+} ion hydrogels, as shown in Fig. 1*F*.

We hypothesized that because each of these single metal ion hydrogels display little overlap in their damping frequency range vs. pH, if we instead include two different metal ions in the same hydrogel we would expect to observe an additive behavior that could significantly broaden the range of mechanical frequencies that match the target damping window. Double metal ion gels studied before have shown that they indeed display a damping behavior roughly captured by double Maxwell-like elements with two distinct relaxation peaks as conceptually illustrated in Fig. 1 *G* and *H*, where the two hypothetical ions from Fig. 1 *D* and *E* are combined into a single hydrogel (see Materials and Methods section for mathematical description).[12] As illustrated in Fig. 1 *H*, the introduction of a second relaxation peak should allow the damping behavior of a single hydrogel to broaden and thereby remain in the target damping window for an increased range of frequencies compared to the single metal ion hydrogels shown in Fig. 1*E*, since the loss factor is no longer a straight line with slope of negative 1. As demonstrated in Fig. 1*I*, we were able to experimentally confirm the predicted additive behavior of single metal ion-induced damping in a quadruple metal ion hydrogel. Specifically, we observed a significantly broadened range of mechanical frequencies that match the target damping window for quadruple metal ion hydrogels formed under various pH conditions, which is a useful demonstration in the development of tunable broadband damping materials. The full frequency sweeps for these quadruple metal ion gels vs. pH are shown in Fig. S3 with the resulting loss factors provided in Fig. S2*E*. Further details, such as the full frequency range tested and additional plots of the target damping range width and location, are given in Fig. S4.

Unfortunately, the application space for these hydrogels is ultimately very limited, as

they rapidly dehydrate and thereby lose their engineered mechanical properties.[13] Here, we explore a potential remedy for this problem. Inspired by other work showcasing how addition of glycerol to hydrogels can improve their mechanical properties, reduce dehydration, and impede freezing, we created a series of metal-coordinate gels with partially substituted glycerol for water as their solvent.[16–20] In addition to the improvements in operational performance properties, glycerol is non-toxic, biodegradable, and produced from renewable sources, ensuring that a substitution of water for glycerol does not make the gels significantly more dangerous or less sustainable.[21] As explained in more detail in the Materials and Methods section, we followed a simple solvent exchange procedure to produce metal-coordinate gels with varying degrees of glycerol content. Briefly, concentrated hydrogels were first established by combining aqueous stock solutions of polymer, metal ion, and sodium hydroxide after which glycerol was added to achieve an initial 62 volume of glycerol in all gels. To control their final glycerol content gels were then placed in individual humidity chambers with a set relative humidity between and to allow the solvent exchange process to reach equilibrium over the course of one week, during which the relative mass changes of the gels were measured daily as an indicator of gel solvation. As shown in Fig. 2 *A*–*D*, the gels with glycerol maintained a final solvated state after equilibrating, whereas control hydrogels with no glycerol rapidly dehydrated. More specifically, as shown in Fig. S5, dependent on the relative humidity of the environment during gel equilibration, gels with glycerol maintain roughly between 0 and 0 of their initial mass after one week, demonstrating that gel glycerol content can indeed be controlled, as shown in Fig. 2*F*, where the final glycerol weight percentages in the gel solvents are estimated, and found to roughly follow prior literature predictions.[22]

Additionally, glycerol acts as an anti-freeze, allowing for the glycerol-containing metal ion cross-linked gels to resist freezing and thereby maintain their desirable properties at much lower temperatures than hydrogels without glycerol. This glycerol-induced freeze resistance is illustrated in Fig. 2*E*, where Differential Scanning Calorimetry (DSC) of the equilibrated

glycerol gels show no thermal transitions when heated from − 0 ° to 0 ° , in sharp contrast to the melting transition observed for fresh control hydrogels. More details about the DSC experiment, including the full heating and cooling cycle, can be seen in Fig. S6. It is important to note that the single metal ion and the quadruple metal ion glycerol-containing gels behave similar with regards to their dehydration and thermal properties.

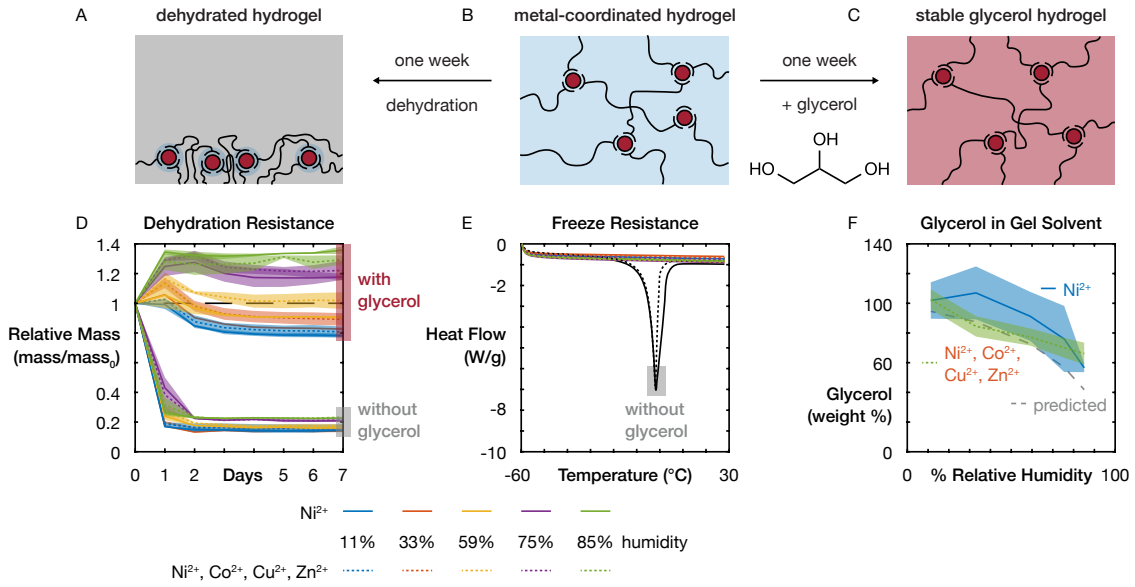

Figure 2: Demonstration of dehydration and freeze resistance in glycerol containing metal cross-linked hydrogels. (*A*) Dehydration rapidly occurs for a (*B*) metal-coordinating hydrogel. (*C*) The addition of glycerol allows for a metal-coordinated gel to remain swollen. (*D*) Experimentally measured changes in relative mass of gels with and without glycerol as a function of relative humidity. Gels without glycerol (i.e. hydrogels) rapidly lose their solvent mass, while gels containing glycerol maintain most of their solvent over a period of one week. The gel's initial mass is denoted as mass_0 and the shaded region provides the range of measurements obtained over two gels. (*E*) Differential scanning calorimetry of glycerol gels equilibrated at a range of humidities and control, glycerol free, hydrogels. Glycerol containing gels do not exhibit a melting transition when heated from − 0 to 0 ° , demonstrating the ability to resist freezing. (*F*) Estimated amount of glycerol in the solvents of gels after one week of equilibration based on measurements shown in *D* and compared to values from literature.[22] Calculated estimates were obtained by comparing the final glycerol gel mass after one week to measured weights of the nonvolatile components of the gel, and assuming any mass in excess was water, as described in the Materials and Methods. A value of 00 means that there is no water remaining, and a value of 0 means that the gel solvent contains no glycerol, only water. The relative humidity of the environment during equilibration of glycerol-containing gels dictates their final solvent composition. Shaded regions illustrate one standard deviation in the calculated value.

Having demonstrated an improved dehydration and freezing resistance for our metal-ion cross-linked hydrogels, we sought to determine how the mechanical properties change with glycerol content. Specifically, we tested the rheological properties of the equilibrated glycerol gels to ensure that the desirable dynamics found in metal ion cross-linked hydrogels are maintained in the glycerol gels. Frequency sweeps for single metal ion Ni^{2+} and quadruple metal ion glycerol gels equilibrated at five different humidities, plus reference control fresh single metal ion and quadruple metal ion hydrogels are given in Fig. S7. From these results, it is important to note that the two lowest humidities used, and , which corresponds to the highest gel glycerol contents, resulted in a waxy material with moduli roughly two orders of magnitude higher than the reference gels and gels equilibrated at higher humidities. Furthermore, these materials had a narrower linear viscoelastic region, meaning they had to be tested at a much lower strain.[23] Because these materials behave significantly different from all other materials in this study, we excluded them from our remaining discussion; however, we believe they are of interest in a further, more specific study. Pictures of all of the gels equilibrated at different humidities are given in Fig. S8, and a video of the gels being handled is freely available online.[24]

The frequency sweeps for the remaining glycerol gels looked qualitatively similar to the reference single ion or quadruple ion hydrogels, showing similar dynamics although with slightly different relaxation timescales and plateau moduli when directly compared in Fig. S9. Lower humidities during gel equilibration consistently resulted in higher gel plateau moduli, a direct result of less total solvent, and therefore more concentrated gel networks with a higher density of elastically active chains. Irrespective of humidity, the relaxation time for the glycerol gels was consistently slower than the reference hydrogels, suggesting that glycerol acts to slow the network dynamics by increasing the solvent viscosity, as expected in a Maxwell model material. The relative humidity gels, displaying the highest moduli, are highlighted specifically in Fig. 3 *A* and *B*.

In addition to frequency sweeps, temperature sweeps were performed on the same set of

gels as shown in Fig. S10, with the relative humidity gels highlighted in Fig. 3*C*. The results of these experiments confirmed the persistence of the gel network dynamics over a wide range of potential operating temperatures. Using the data from both the frequency and temperature sweeps, we can now understand the damping properties in the glycerol gels and determine if quadruple metal ion gels dampen over a larger frequency and temperature range in comparison to single metal ion gels. Additionally, we can look to see if glycerol content, as dictated by the gel equilibration humidity, impacts damping properties. This is done similarly to the previously examined hydrogels, by first plotting the loss factor for the

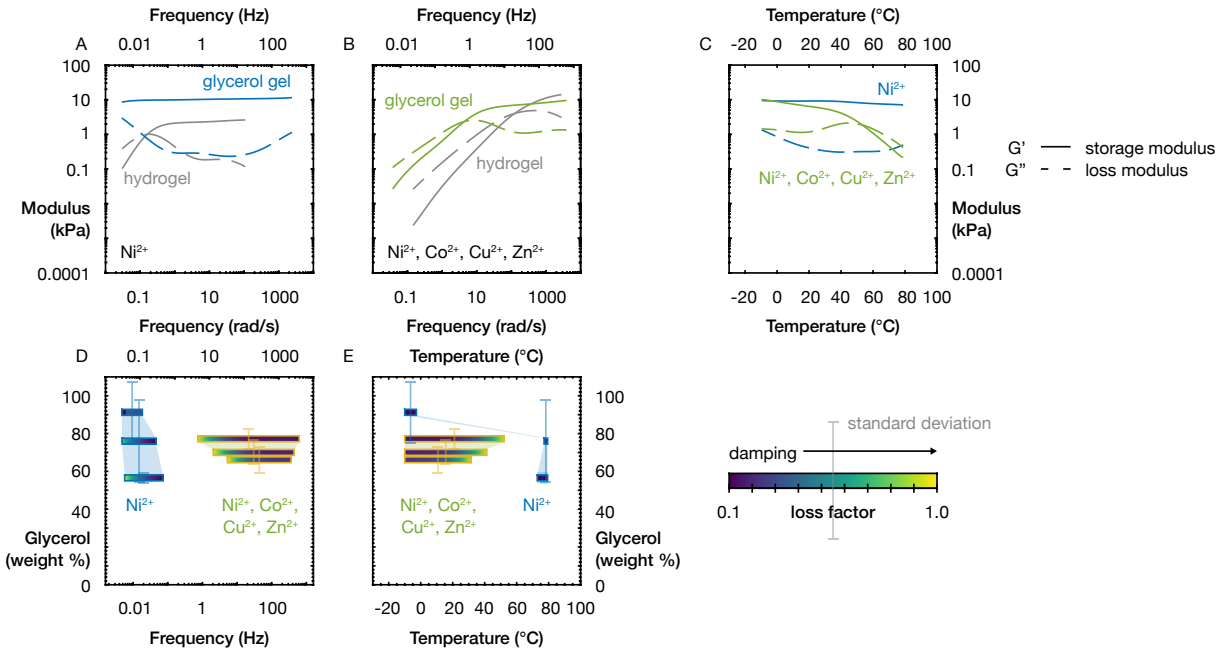

Figure 3: Examination of rheological and damping properties of glycerol containing metal-coordinated hydrogels. (*A*) Both a single metal ion and (*B*) multiple metal ion glycerol gel aged at relative humidity exhibit similar, but slower, rheological behavior compared to a reference, freshly prepared, glycerol free hydrogel prepared with an equal volume of water instead of glycerol for comparison. (*C*) Glycerol gel rheology can be measured between $-\ 0\,^{\circ}$ and $0\,^{\circ}$ demonstrating a large thermal tolerance for the material. Glycerol gel data in *A*–*C* is from the relative humidity gels. (*D*) Experimentally determined frequency ranges and (*E*) temperature ranges matching the target damping window, as a function of glycerol content (see Fig. 2*F*) for both single metal ion Ni^{2+} glycerol gels and multiple metal ion Ni^{2+}, Co^{2+}, Cu^{2+}, and Zn^{2+} glycerol gels show wider ranging damping properties for the multiple metal ion gels. The error bars across the color bars in *D* and *E* indicate the standard deviation of the estimate of glycerol content from Fig. 2*F*.

gels, given in Fig. S11, then extracting the portion of the loss factor that lies in the target damping window range between 0.1 and 1, and then plotting these values as a color bar in Fig. 3*D* for the frequency sweeps and Fig. 3*E* for the temperature sweeps, as a function of gel glycerol content (see Fig. 2*F* for the connection between gel humidity and glycerol content and Fig. S12 for the damping data plotted against humidity). Doing so clearly demonstrates that the quadruple ion gels have a larger frequency and temperature damping range in comparison to the single metal ion gels. The position of the damping region appears to be largely dictated by the pH of the original hydrogels, which are all between 7.5 and 8.5, and follows from the hydrogel results vs. pH given in Fig. 1 *F* and *I*. The frequency damping position seemed to slightly increase in correlation with decreasing glycerol content, in agreement with the gels relaxing faster as the humidity and thereby the water portion of gel solvent increases; however, trends in the frequency and temperature damping width vs. glycerol content were difficult to elucidate given that the damping range intersects with the limits we experimentally accessed, as shown in Fig. S13.

Conclusions

Several of the principles demonstrated in this study should be directly applicable to the future development of vibration damping materials and metal ion cross-linked hydrogels for other applications. For example, the simple method of a solvent exchange in a humidity chamber to produce metal coordinated glycerol gels should be directly applicable to future work in designing self-healing, energy dissipating, tough gels, as the use of glycerol enhances thermal properties by both eliminating dehydration and resisting freezing, thereby vastly expanding the application space for these materials. Importantly, with a minimum humidity requirement, the glycerol gel mechanical properties largely mirror the properties in the pure hydrogels, thereby allowing the design principles developed over the past decade in metal ion cross-linked hydrogels to be translated directly to this next generation material. As a test of

this translation, we demonstrated that expanded vibration damping of quadruple metal ion gels in comparison to single metal ion gels can be directly extended into metal ion cross-linked glycerol gels. Important future studies could include how well pH control extends into the glycerol gels, further characterization and study of the high glycerol content, low humidity gels, and making these materials with a different ligand such as catechol or nitrocatechol. We anticipate that the materials developed in this study, or future extensions thereof, can find specific applications as broadband vibration dampeners in environmentally uncontrolled performance scenarios such as wing vibration damping during operation of Unmanned Aerial Vehicles.[25–27]

Materials and Methods

Materials

All chemicals were purchased from Millipore Sigma, except for the polymer, which was purchased from JenKem USA.

Synthesis of 4-arm star histidine PEG polymer

Coupling of the histidine ligand to the polymer was performed by slightly modifying a procedure used elsewhere.[28,29] Briefly, 4-arm star, 0 PEG, terminated with $NH_2 \cdot HCl$ (four equivalence per polymer), was mixed with 1.5 equivalence Boc-His(Trt)-OH and 1.5 equivalence BOP reagent, and dissolved in a minimal amount of dichloromethane. 535 equivalence of N,N-Diisopropylethylamine (DIPEA) was then added and the reaction proceeded under nitrogen overnight. Purification was performed by precipitation once in ether, 3 times in $-\ 0\,^\circ$ methanol, and then once in ether before being dried under vacuum. The product was then cleaved using a solution of trifluoracetic acid, triisopropylsilane, and water by volume for 2 hours. An equal volume of methanol was then added to the cleavage solution, and the solvent was removed using a rotary evaporator. The final product

Table 1: Concentration of stock 4-arm histidine solution via NMR using internal formate standard

Integration Limits (ppm)	Integration Values
8.91 - 8.20	1.54
7.65 - 7.22	1.00
4.30 - 4.16	0.97
Formate Integration	0.54

was purified by dissolving it in methanol and precipitated in ether 3 times. The cleaved product was then vacuum dried, dissolved in water, and lyophilized before being stored in a $-0\,^{\circ}$ freezer. ^{1}H-NMR (500 MHz, D_2O): (ppm) 8.59 (s, 4 H), 7.41 (s, 4 H), 4.23 (t, 0 , 4 H), 4.08–3.28 (m, 984 H). MALDI-TOF in sinapinic acid matrix gives M_n = 10 644 Da. Coupling efficiency estimated to be 91.6 %. See Fig. S14 for characterization data.

Hydrogel formation and mixing

Stock solutions were made of 4 M NaOH and 1 M cross-linking ion salts $NiCl_2 \cdot 6\,H_2O$, $CoCl_2 \cdot 6\,H_2O$, $CuCl_2 \cdot 2\,H_2O$ and $ZnCl_2$. A stock solution of 4-arm 10 kDa histidine was made, and the concentration of histidine was determined using ^{1}H-NMR and a 0.0444 M formate ion standard to be 0.082 M, as shown in Table 1, which gives the averaged ^{1}H-NMR results. A 0.04 M histidine hydrogel was formed by modifying the method described elsewhere.[8,29] 97.6 µL of stock 4-arm histidine was dispensed onto Parafilm® along with a 1 M stock Ni^{2+}, Co^{2+}, Cu^{2+} or Zn^{2+}, solution, a 4 M NaOH solution, and water so that the final hydrogel volume would be 200 µL. The total salt ion concentration was fixed at 0.08 M, representing a value twice the ligand concentration. If multiple metal ions were used, those drops were then mixed together. Next, the salt drop was mixed with the polymer drop, and this combined drop was mixed with the NaOH drop and finally the water drop using a spatula. The resulting mixture was then homogenized by mixing with the spatula and by kneading the material by folding the Parafilm®.

Glycerol gels and reference glycerol free hydrogels formation and mixing

Glycerol gels, and gels made for the dehydration study, were made slightly differently. 97.6 µL of stock 4-arm histidine was dispensed onto Parafilm® along with a 16 µL of total stock ion salt and 9 µL NaOH solution. The total salt ion concentration represents a value twice the ligand concentration. If multiple metal ions were used, those drops were then mixed together. Next, the salt drop was mixed with the polymer drop, and this combined drop was mixed with the NaOH drop using a spatula. Finally, either 200 µL of glycerol or water was added to the gels before they were aged in their humidity chambers, resulting in an initial concentration of 62 % glycerol by volume ($\frac{200}{9 \quad 1 \quad 9 \quad 200}$). Reference rheology was performed on freshly prepared glycerol free hydrogels of this concentration (200 µL water added instead of glycerol) for a proper comparison between hydrogels and aged glycerol gels.

Dehydration Study

Gels were aged in humidity chambers consisting of 1 gallon plastic jars containing a 50 mL centrifuge tube taped to the inside wall of the jar containing 30 mL of saturated salt solution. The saturated salt solutions that were used to control the humidity are listed in Table 2.[30] The mass of the gels were measured daily over the course of one week to measure the relative mass loss as a function of time in different relative humidities. The weight percent of glycerol in the solvent at an aging time of 7 days was determined by measuring the hydrated and dehydrated mass of each component (polymer, salt, and base stock solutions) to extract the solid mass, and water mass in the initial gels. The amount of water in the glycerol gels after 7 days was determined by assuming the remaining gel mass consists of the nonvolatile components (the solid, or dehydrated masses, and glycerol) with any leftover being attributed to remaining water. These calculations were compared to values from literature.[22]

Table 2: Humidity control via saturated salt solutions[30]

Saturated Salt Solution	Relative Humidity
LiCl	11.3%
$MgCl_2$	33.1%
NaBr	59.1%
NaCl	75.5%
KCl	85.1%

Rheological testing of hydrogels

The resulting hydrogels were measured for their viscoelastic properties and pH. The gels were loaded onto an MCR 302 stress-controlled rheometer from Anton Paar and tested using a 10 mm diameter, parallel plate geometry with a 400 µm gap and sealed with mineral oil to prevent dehydration. Frequency sweeps for hydrogels were performed from 100–0.1 rad/s at temperatures of 5, 15, 25, and 35 °C at a strain amplitude of 5 %. Frequency sweeps for glycerol gels and reference hydrogels were performed from 100–0.1 rad/s at temperatures of − 0, − , 5, 15, 25, and 35 °C at a strain amplitude of 5 % for gels aged in 59.1, 75.5, and 85.1 % humidity and at a strain amplitude of 0.1 % for gels aged in 11.3 and 33.1 % humidity. After the 35 °C frequency sweep, a strain sweep was performed at 25 °C from 0.1–500 % strain at a frequency of 10 rad/s to confirm the linear viscoelastic region for the gels. For the glycerol gels aged in 11.3 and 33.1 % humidity, a strain sweep was performed at a lower amplitude range of 0.01–10 %. Time temperature superposition was used to combine the frequency sweep results at the different temperatures to the 25 °C measurement, and the master frequency sweep was fitted using pyReSpect.[31] For the aged glycerol gels and reference hydrogels, a temperature sweep was performed from −10 °C–120 °C at 40 rad/s and the same strain amplitudes used for the frequency sweeps. For frequency sweeps of the hydrogels, see Fig. S1 and S3. For frequency and temperature sweeps of the hydrogels, see Fig. S7 and S10. The damping range for the gels was determined as the frequency or temperature range where the gels loss factor was between 0.1–1. The pH of the gels were determined using a SoilStik pH meter from FieldScout on the portion of the gel trimmed

from the rheometer.

Differential Scanning Calorimetry

Differential Scanning Calorimetry (DSC) was performed on the aged glycerol gels and fresh reference hydrogels using a TA Instruments Discovery DSC. 5 mg–10 mg of gel was loaded into a Tzero pan, covered with a Tzero hermetic lid, and crimped. The pan was then loaded into the instrument, equilibrated to −60 °C, and then cycled up and down between −60 °C–30 °C 3 times at a heating/cooling rate of 10 °C/min and isothermal rests of 1 min at the end of each thermal ramp. The second cycle is plotted in Fig. 2 and S6.

Hypothetical Frequency Sweeps

To produce the hypothetical single metal ion frequency sweeps, we used Eqn. 1 to plot the storage modulus and Eqn. 2 to plot the loss modulus, where τ is the relaxation time, is the angular frequency, and $_u$ is the plateau modulus. For each single metal ion gel, we changed the relaxation time τ to represent an independent relaxation time associated with each metal ion.

$$' \quad {}_u \frac{\tau^2 \ ^2}{\tau^2 \ ^2} \tag{1}$$

$$ {}_u \frac{\tau}{\tau^2 \ ^2} \tag{2}$$

To model the hypothetical double metal gel, we averaged the behavior from the single metal ion gels using Eqn. 3 for the storage modulus and Eqn. 4 for the loss modulus. The subscripts and refer to each single metal ion gel with individual relaxation timescale τ.

$$' \quad \frac{' \quad '}{} \tag{3}$$

$$\frac{}{} \tag{4}$$

Acknowledgements

DISTRIBUTION STATEMENT A. Approved for public release. Distribution is unlimited. This material is based upon work supported by the United States Air Force under Air Force Contract No. FA8702-15-D-0001. Any opinions, findings, conclusions or recommendations expressed in this material are those of the author(s) and do not necessarily reflect the views of the United States Air Force.

References

(1) Chung, D. D. Review: Materials for vibration damping. *J. Mater. Sci.* **2001**, *36*, 5733–5737, DOI: 10.1023/A:1012999616049.

(2) Vaccaro, E.; Waite, J. H. Yield and Post-Yield Behavior of Mussel Byssal Thread: A Self-Healing Biomolecular Material. *Biomacromolecules* **2001**, *2*, 906–911, DOI: 10.1021/bm0100514.

(3) Harrington, M. J.; Masic, A.; Holten-Andersen, N.; Waite, J. H.; Fratzl, P. Iron-Clad Fibers: A Metal-Based Biological Strategy for Hard Flexible Coatings. *Science (80-.).* **2010**, *328*, 216–220, DOI: 10.1126/science.1181044.

(4) Schmitt, C. N. Z.; Politi, Y.; Reinecke, A.; Harrington, M. J. Role of sacrificial protein-metal bond exchange in mussel byssal thread self-healing. *Biomacromolecules* **2015**, *16*, 2852–2861, DOI: 10.1021/acs.biomac.5b00803.

(5) Priemel, T.; Degtyar, E.; Dean, M. N.; Harrington, M. J. Rapid self-assembly of complex biomolecular architectures during mussel byssus biofabrication. *Nat. Commun.* **2017**, *8*, 14539, DOI: 10.1038/ncomms14539.

(6) George, S.; Pirie, B.; Coombs, T. The kinetics of accumulation and excretion of ferric

hydroxide in Mytilus edulis (I.) and its distribution in the tissues. *J. Exp. Mar. Bio. Ecol.* **1976**, *23*, 71–84, DOI: 10.1016/0022-0981(76)90086-1.

(7) Schmitt, C. N. Z.; Winter, A.; Bertinetti, L.; Masic, A.; Strauch, P.; Harrington, M. J. Mechanical homeostasis of a DOPA-enriched biological coating from mussels in response to metal variation. *J. R. Soc. Interface* **2015**, *12*, 20150466, DOI: 10.1098/rsif.2015.0466.

(8) Holten-Andersen, N.; Harrington, M. J.; Birkedal, H.; Lee, B. P.; Messersmith, P. B.; Lee, K. Y. C.; Waite, J. H. pH-induced metal-ligand cross-links inspired by mussel yield self-healing polymer networks with near-covalent elastic moduli. *Proc. Natl. Acad. Sci.* **2011**, *108*, 2651–2655, DOI: 10.1073/pnas.1015862108.

(9) Fullenkamp, D. E.; He, L.; Barrett, D. G.; Burghardt, W. R.; Messersmith, P. B. Mussel-Inspired Histidine-Based Transient Network Metal Coordination Hydrogels. *Macromolecules* **2013**, *46*, 1167–1174, DOI: 10.1021/ma301791n.

(10) Zheng, S. Y.; Ding, H.; Qian, J.; Yin, J.; Wu, Z. L.; Song, Y.; Zheng, Q. Metal-Coordination Complexes Mediated Physical Hydrogels with High Toughness, Stick-Slip Tearing Behavior, and Good Processability. *Macromolecules* **2016**, *49*, 9637–9646, DOI: 10.1021/acs.macromol.6b02150.

(11) Holten-Andersen, N.; Jaishankar, A.; Harrington, M. J.; Fullenkamp, D. E.; DiMarco, G.; He, L.; McKinley, G. H.; Messersmith, P. B.; Lee, K. Y. C. Metal-coordination: using one of nature's tricks to control soft material mechanics. *J. Mater. Chem. B* **2014**, *2*, 2467, DOI: 10.1039/c3tb21374a.

(12) Grindy, S. C.; Learsch, R.; Mozhdehi, D.; Cheng, J.; Barrett, D. G.; Guan, Z.; Messersmith, P. B.; Holten-Andersen, N. Control of hierarchical polymer mechanics with bioinspired metal-coordination dynamics. *Nat. Mater.* **2015**, *14*, 1210–1216, DOI: 10.1038/nmat4401.

(13) Kim, S.; Peterson, A. M.; Holten-Andersen, N. Enhanced Water Retention Maintains Energy Dissipation in Dehydrated Metal-Coordinate Polymer Networks: Another Role for Fe-Catechol Cross-Links? *Chem. Mater.* **2018**, *30*, 3648–3655, DOI: 10.1021/acs.chemmater.7b05246.

(14) Barrett, D. G.; Fullenkamp, D. E.; He, L.; Holten-Andersen, N.; Lee, K. Y. C.; Messersmith, P. B. PH-based regulation of hydrogel mechanical properties through mussel-inspired chemistry and processing. *Adv. Funct. Mater.* **2013**, *23*, 1111–1119, DOI: 10.1002/adfm.201201922.

(15) Grindy, S. C.; Holten-Andersen, N. Bio-inspired metal-coordinate hydrogels with programmable viscoelastic material functions controlled by longwave UV light. *Soft Matter* **2017**, *13*, 4057–4065, DOI: 10.1039/C7SM00617A.

(16) Xue, S.; Wu, Y.; Guo, M.; Xia, Y.; Liu, D.; Zhou, H.; Lei, W. Self-healable poly(acrylic acid-: Co -maleic acid)/glycerol/boron nitride nanosheet composite hydrogels at low temperature with enhanced mechanical properties and water retention. *Soft Matter* **2019**, *15*, 3680–3688, DOI: 10.1039/c9sm00179d.

(17) Pan, X.; Wang, Q.; Ning, D.; Dai, L.; Liu, K.; Ni, Y.; Chen, L.; Huang, L. Ultraflexible Self-Healing Guar Gum-Glycerol Hydrogel with Injectable, Antifreeze, and Strain-Sensitive Properties. *ACS Biomater. Sci. Eng.* **2018**, *4*, 3397–3404, DOI: 10.1021/acsbiomaterials.8b00657.

(18) Han, L.; Liu, K.; Wang, M.; Wang, K.; Fang, L.; Chen, H.; Zhou, J.; Lu, X. Mussel-Inspired Adhesive and Conductive Hydrogel with Long-Lasting Moisture and Extreme Temperature Tolerance. *Adv. Funct. Mater.* **2018**, *28*, 1–12, DOI: 10.1002/adfm.201704195.

(19) Qin, Z.; Dong, D.; Yao, M.; Yu, Q.; Sun, X.; Guo, Q.; Zhang, H.; Yao, F.; Li, J. Freezing-Tolerant Supramolecular Organohydrogel with High Toughness, Thermoplasticity, and

Healable and Adhesive Properties. *ACS Appl. Mater. Interfaces* **2019**, *11*, 21184–21193, DOI: 10.1021/acsami.9b05652.

(20) Xia, Y.; Wu, Y.; Yu, T.; Xue, S.; Guo, M.; Li, J.; Li, Z. Multifunctional Glycerol-Water Hydrogel for Biomimetic Human Skin with Resistance Memory Function. *ACS Appl. Mater. Interfaces* **2019**, *11*, 21117–21125, DOI: 10.1021/acsami.9b05554.

(21) Wolfson, A.; Dlugy, C.; Shotland, Y. Glycerol as a green solvent for high product yields and selectivities. *Environ. Chem. Lett.* **2007**, *5*, 67–71, DOI: 10.1007/s10311-006-0080-z.

(22) Glycerine Producers' Association, *Physical Properties of Glycerine and Its Solutions*; 1963; pp 1–27.

(23) Dimitriou, C. J. The rheological complexity of waxy crude oils: Yielding, thixotropy and shear heterogeneities. *Massachusetts Inst. Technol.* **2008**,

(24) Cazzell, S. A. Movie of metal ion cross-linked glycerol gels aged at different relative humidities. 2020; http://doi.org/10.5281/zenodo.3740867.

(25) Zhou, X.; Yu, D.; Shao, X.; Zhang, S.; Wang, S. Research and applications of viscoelastic vibration damping materials: A review. *Composite Structures* **2016**, *136*, 460 – 480, DOI: https://doi.org/10.1016/j.compstruct.2015.10.014.

(26) Plasencia, G. N. M.; Rodríguez, M. T.; Rivera, S. C.; Ángela Hernández López, Modelling and Analysis of Vibrations in a UAV Helicopter with a Vision System. *International Journal of Advanced Robotic Systems* **2012**, *9*, 220, DOI: 10.5772/52761.

(27) Goyal, C.; Varun K.C, D.; Sarweswaran, R.; Manivannan, P. Vibration resistance biohybrid composite material for UAV application. *Materials Today: Proceedings* **2020**, DOI: https://doi.org/10.1016/j.matpr.2020.08.050.

(28) Grindy, S. C.; Lenz, M.; Holten-Andersen, N. Engineering Elasticity and Relaxation Time in Metal-Coordinate Cross-Linked Hydrogels. *Macromolecules* **2016**, *49*, 8306–8312, DOI: 10.1021/acs.macromol.6b01523.

(29) Cazzell, S. A.; Holten-Andersen, N. Expanding the stoichiometric window for metal cross-linked gel assembly using competition. *Proc. Natl. Acad. Sci.* **2019**, *116*, 21369–21374, DOI: 10.1073/pnas.1906349116.

(30) Greenspan, L. Humidity Fixed Points of Binary Saturated Aqueous Solutions. *J. Res. Natl. Bur. Stand. Phys. Chem.* **1977**, *81A*, 89–96.

(31) Shanbhag, S. pyReSpect: A Computer Program to Extract Discrete and Continuous Spectra from Stress Relaxation Experiments. *Macromol. Theory Simulations* **2019**, *28*, 1–10, DOI: 10.1002/mats.201900005.

Supporting Information

Demonstration of environmentally stable, broadband energy dissipation via multiple metal cross-linked glycerol gels

Seth Allen Cazzell, Bradley Duncan, Richard Kingsborough, and Niels Holten-Andersen

holten@mit.edu

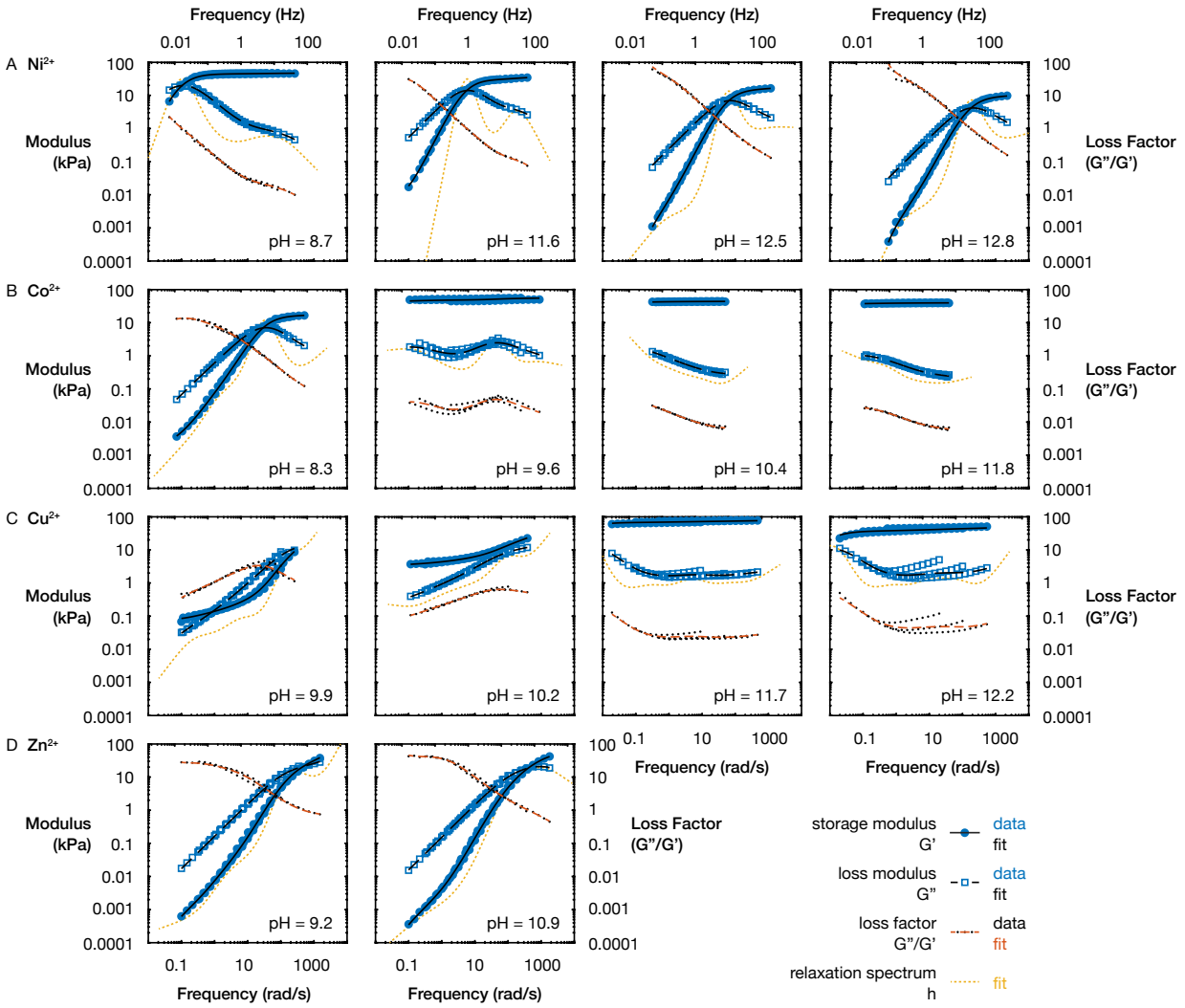

Figure S1: Frequency sweeps of single metal ion hydrogels. Rheological behavior vs. pH for single metal ion (*A*) Ni^{2+}, (*B*) Co^{2+}, (*C*) Cu^{2+}, and (*D*) Zn^{2+} coordinated hydrogels.

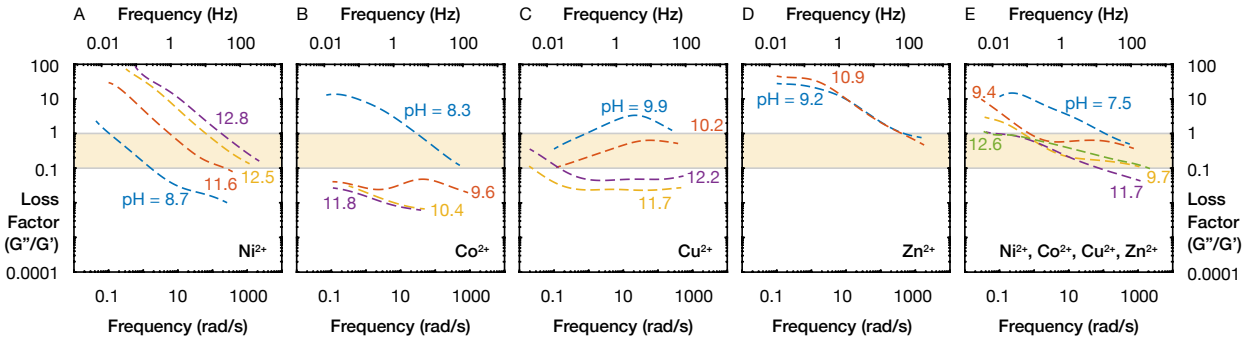

Figure S2: Loss factor of single and multiple metal ion cross-linked hydrogels vs. pH. Rheological behavior vs. pH for single metal ion (*A*) Ni^{2+}, (*B*) Co^{2+}, (*C*) Cu^{2+}, and (*D*) Zn^{2+} coordinated hydrogels and (*E*) multiple metal ion gels.

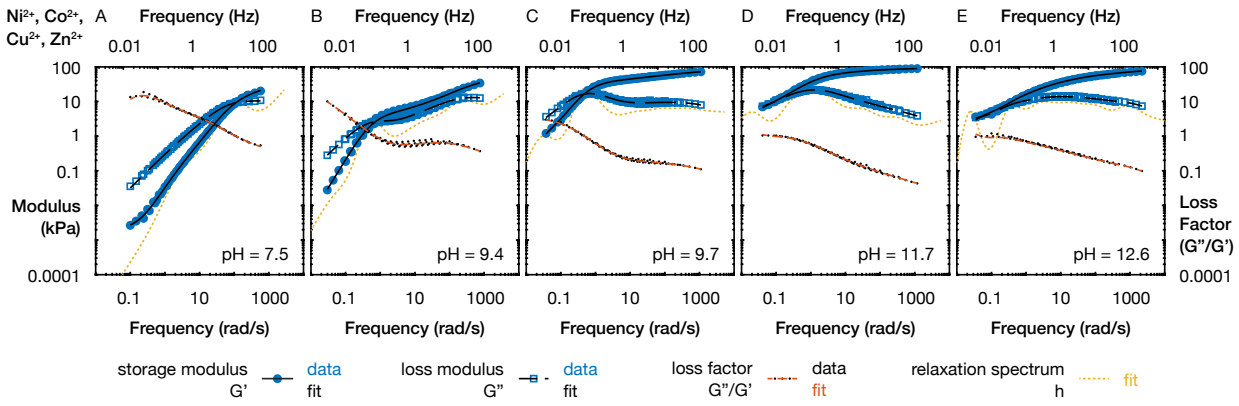

Figure S3: Frequency sweeps of multiple metal ion hydrogels. (*A*-*E*) Rheological behavior vs. pH for multiple metal ion Ni^{2+}, Co^{2+}, Cu^{2+}, Zn^{2+} coordinated hydrogels.

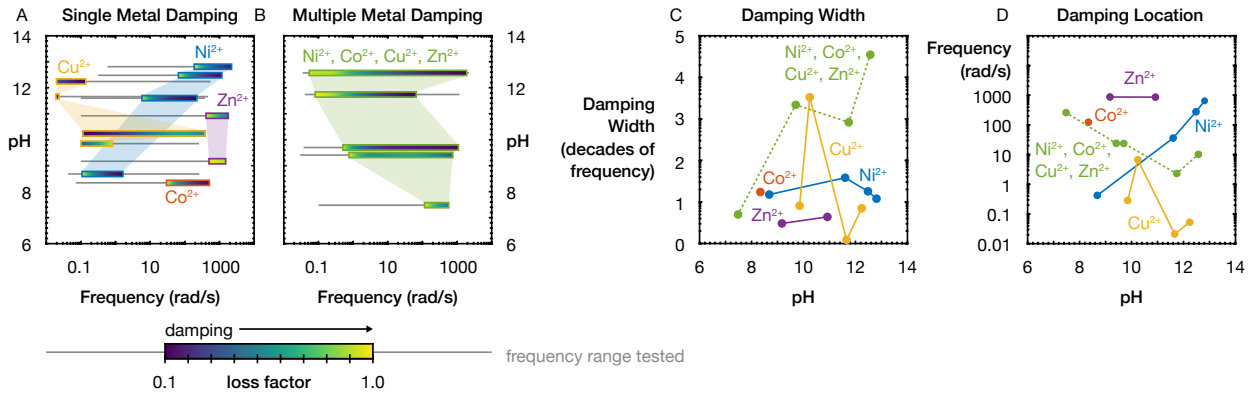

Figure S4: Damping properties of single metal vs. multiple metal ion cross-linked hydrogels. (*A*) Target damping frequency range for single metal ion gels and (*B*) multiple metal ion gels as shown in Fig. 1*F*, but with the full range of frequencies tested additionally shown here. (*C*) Width of the frequency range matching the target damping window of single and multiple metal ion hydrogels as a function of pH. (*D*) Midpoint location of the frequency range matching the target damping window as indicated by the midpoint of damping frequency of single and multiple metal ion hydrogels as a function of pH.

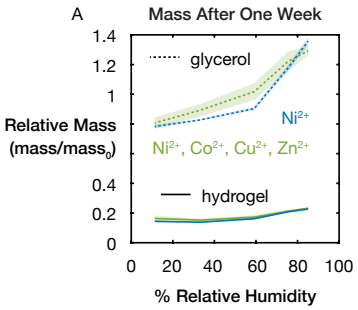

Figure S5: Relative mass change after one week of aging in a range of relative humidities. (*A*) Single metal and multiple metal ion hydrogels maintain roughly 20% of their initial mass. Glycerol containing hydrogels maintain between 80% and 140% of their initial mass. Both classes of materials show a stronger correlation of increasing mass maintained as a function of increasing humidity.

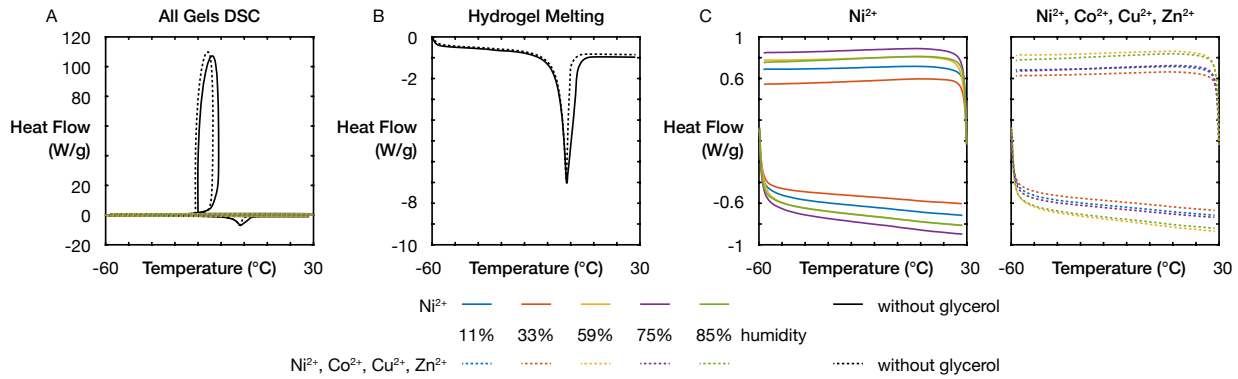

Figure S6: Thermal properties of glycerol hydrogels aged in a range of relative humidities. (*A*) Second heating and cooling cycles show strong melting and freezing transitions for the glycerol free gels, but no transition for any of the gels with glycerol. (*B*) Melting enthalpy peaks for reference hydrogels show freezing around -1°C for both a single metal ion Ni^{2+} gel and a multiple metal ion Ni^{2+}, Co^{2+}, Cu^{2+}, Zn^{2+} gel. (*C*) Full second cooling and heating cycles for both the single metal ion Ni^{2+} and quadruple metal ion Ni^{2+}, Co^{2+}, Cu^{2+}, Zn^{2+} glycerol gels show no thermal transition.

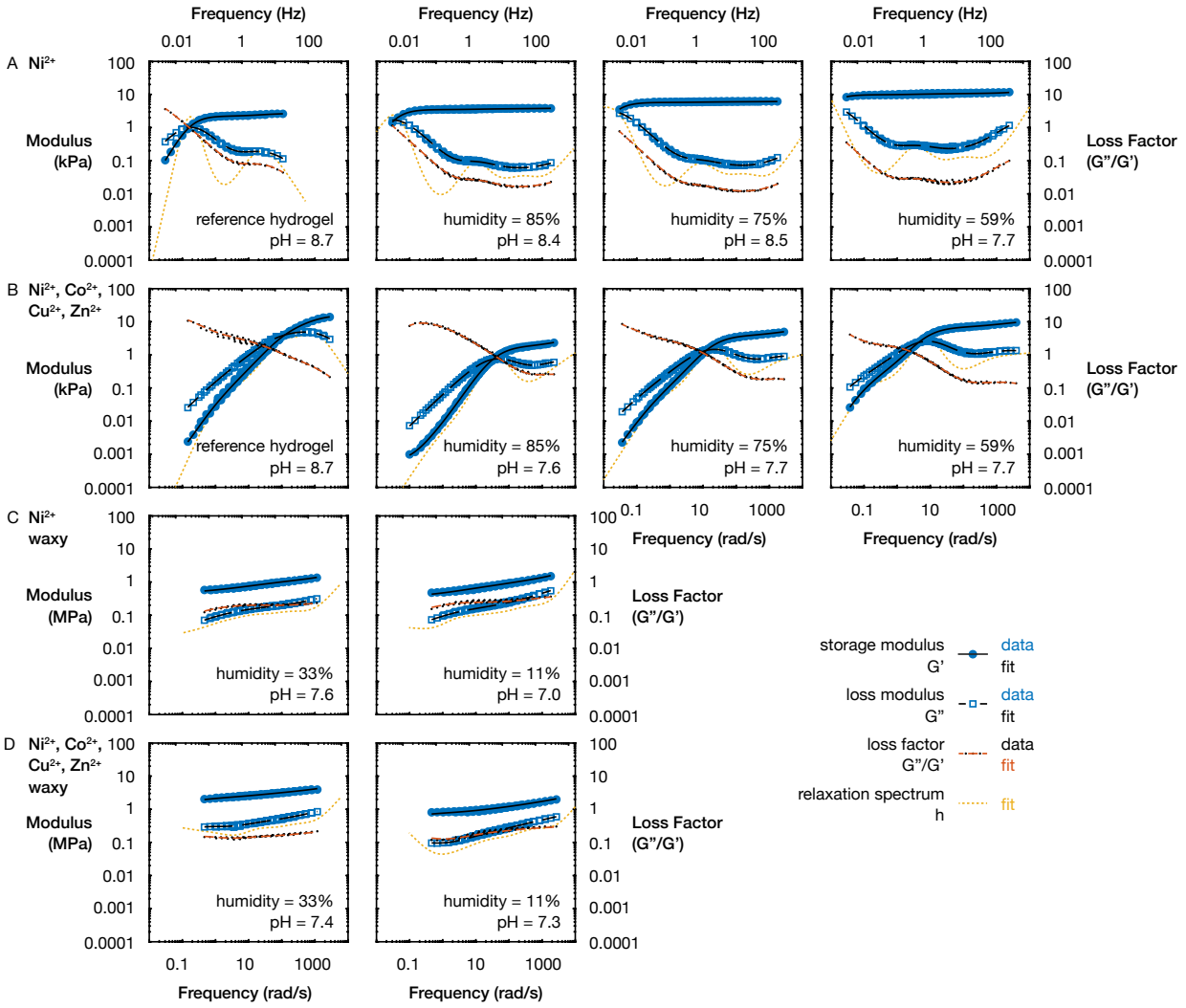

Figure S7: Glycerol containing metal cross-linked hydrogels frequency sweeps. (A) Single metal ion Ni^{2+} and (B) multiple metal ion Ni^{2+}, Co^{2+}, Cu^{2+}, Zn^{2+} frequency sweeps of fresh reference glycerol free hydrogel and glycerol containing gels aged at 85%, 75%, and 59% humidity. Frequency sweep for (C) single metal ion and (D) multiple metal ion glycerol gels aged at 33% and 11% humidity resulted in a waxy material. Note the scale of the modulus axes in (A) and (B) is in kPa and in (C) and (D) is in MPa.

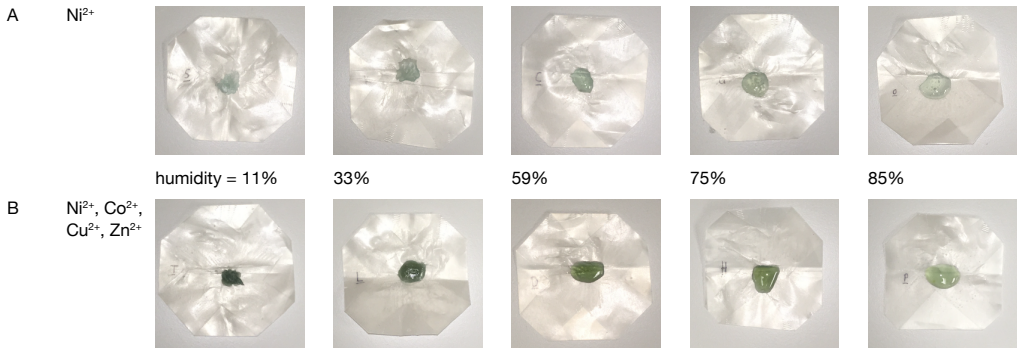

Figure S8: Images of single and multiple metal ion glycerol gels. (*A*) Ni^{2+} single metal ion and (*B*) Ni^{2+} Co^{2+}, Cu^{2+}, Zn^{2+} multiple metal ion glycerol gels aged at different relative humidities.

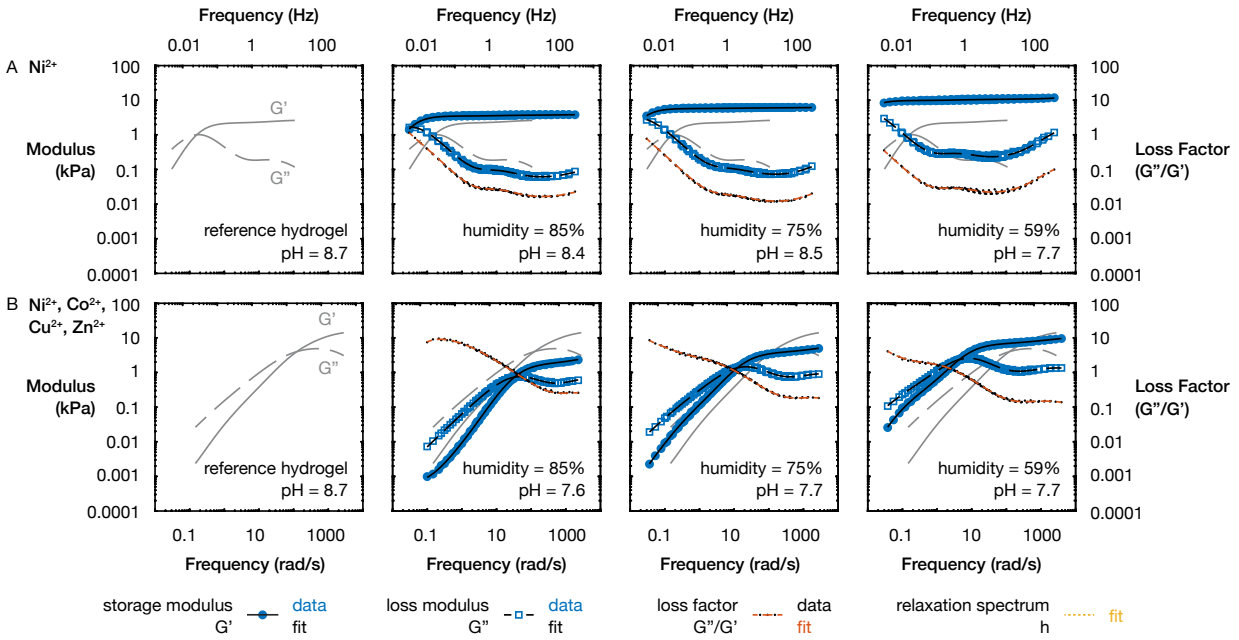

Figure S9: Comparing the viscoelastic behavior of glycerol containing and glycerol free metal ion cross-linked gels. Comparison of frequency sweep of glycerol free vs. glycerol containing gels for (A) single metal ion Ni^{2+}gels and (B) multiple metal ion Ni^{2+}, Co^{2+}, Cu^{2+}, Zn^{2+} gels shows glycerol results in a slower relaxation.

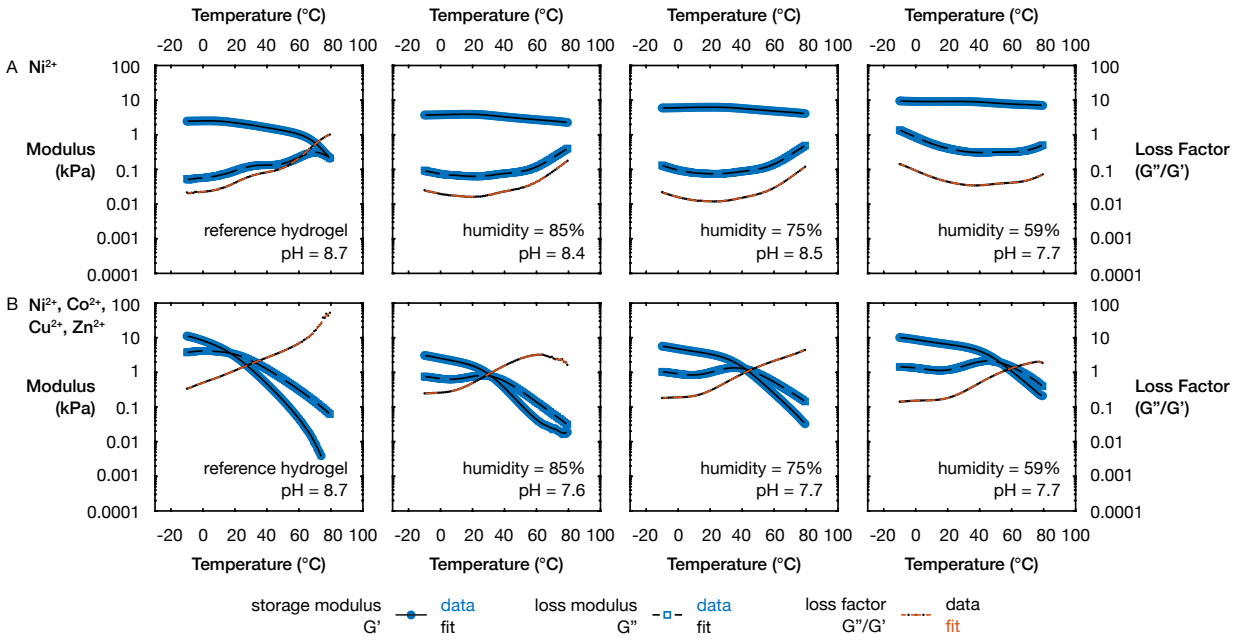

Figure S10: Comparing the rheological behavior of glycerol containing and glycerol free metal ion cross-linked gels as a function of temperature. Comparison of temperature sweep of glycerol free and glycerol containing gels for (A) single metal ion Ni^{2+}gels and (B) multiple metal ion Ni^{2+}, Co^{2+}, Cu^{2+}, Zn^{2+} gels.

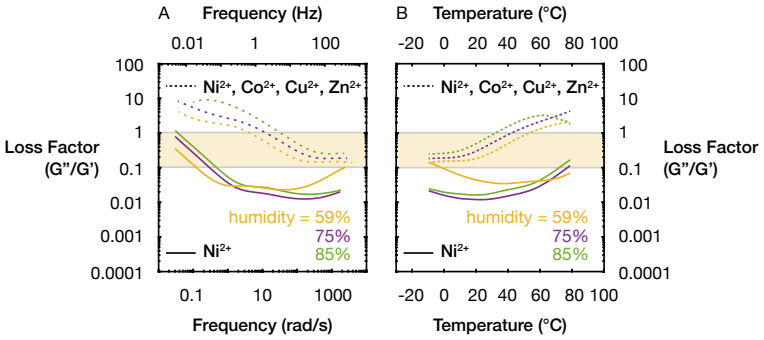

Figure S11: Plots of the loss factor vs. frequency and vs. temperature for glycerol containing hydrogels. (*A*) Loss factor vs. frequency demonstrates that multiple metal ion gels remain in the damping range for a larger range of frequencies compared to the single metal ion gels. (*B*) Loss factor vs. temperature demonstrates that multiple metal ion gels remain in the damping range for a larger range of temperatures compared to the single metal ion gels.

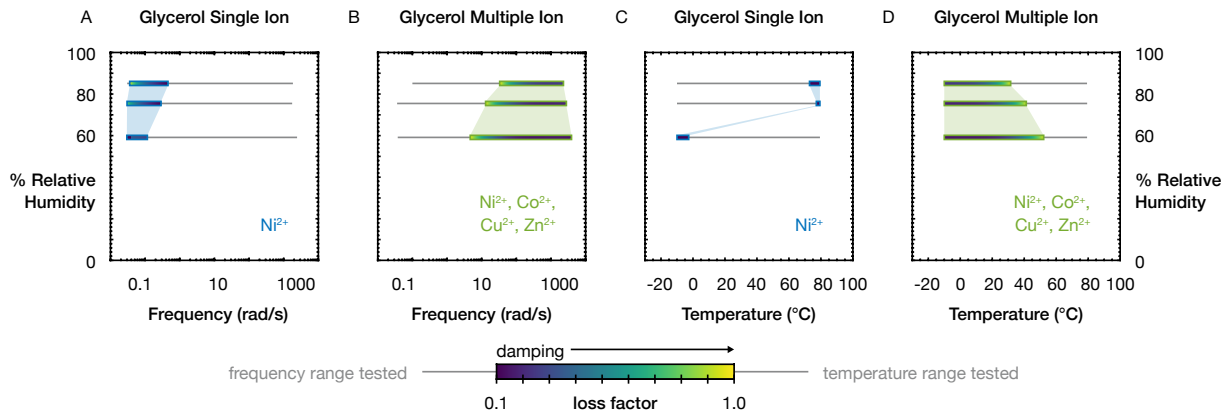

Figure S12: Damping properties of glycerol containing metal-coordinated hydrogels as a function of humidity. (A) Damping is observed for single metal ion Ni^{2+} gels over a narrow frequency range, while damping is observed over a larger frequency range for (B) multiple metal ion Ni^{2+}, Co^{2+}, Cu^{2+}, Zn^{2+} gels. (C) Damping is observed for single metal ion Ni^{2+} gels over a narrow temperature range, while damping is observed over a larger temperature range for (D) multiple metal ion Ni^{2+}, Co^{2+}, Cu^{2+}, Zn^{2+} gels.

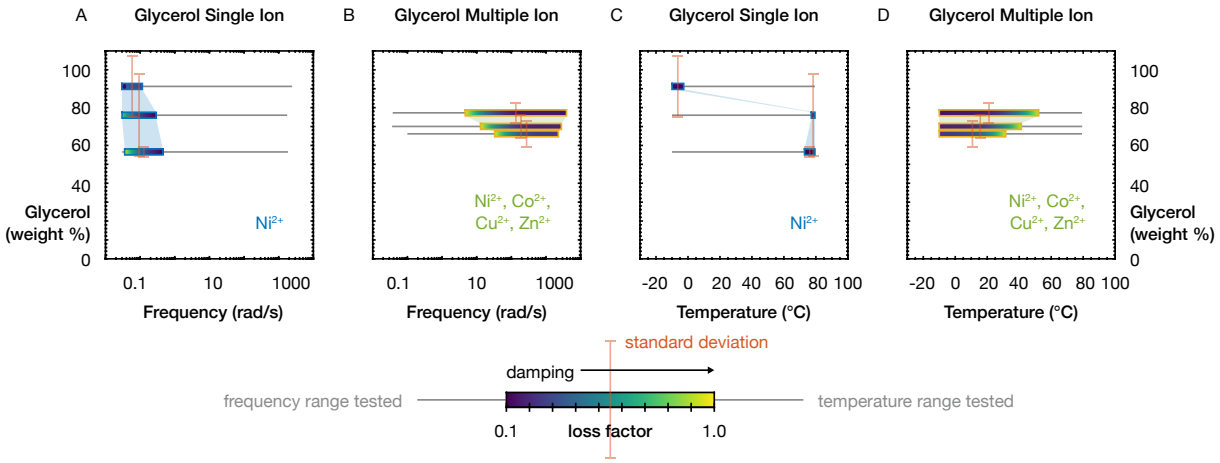

Figure S13: Damping properties of glycerol containing metal-coordinated hydrogels as a function glycerol content. (*A*) Damping is observed for single metal ion Ni^{2+} gels over a narrow frequency range, while damping is observed over a larger frequency range for (*B*) multiple metal ion Ni^{2+}, Co^{2+}, Cu^{2+}, Zn^{2+} gels. (*C*) Damping is observed for single metal ion Ni^{2+} gels over a narrow temperature range, while damping is observed over a larger temperature range for (*D*) multiple metal ion Ni^{2+}, Co^{2+}, Cu^{2+}, Zn^{2+} gels. The error bars across the color bars indicate the standard deviation of the estimate of glycerol content from Fig. 2*F*.

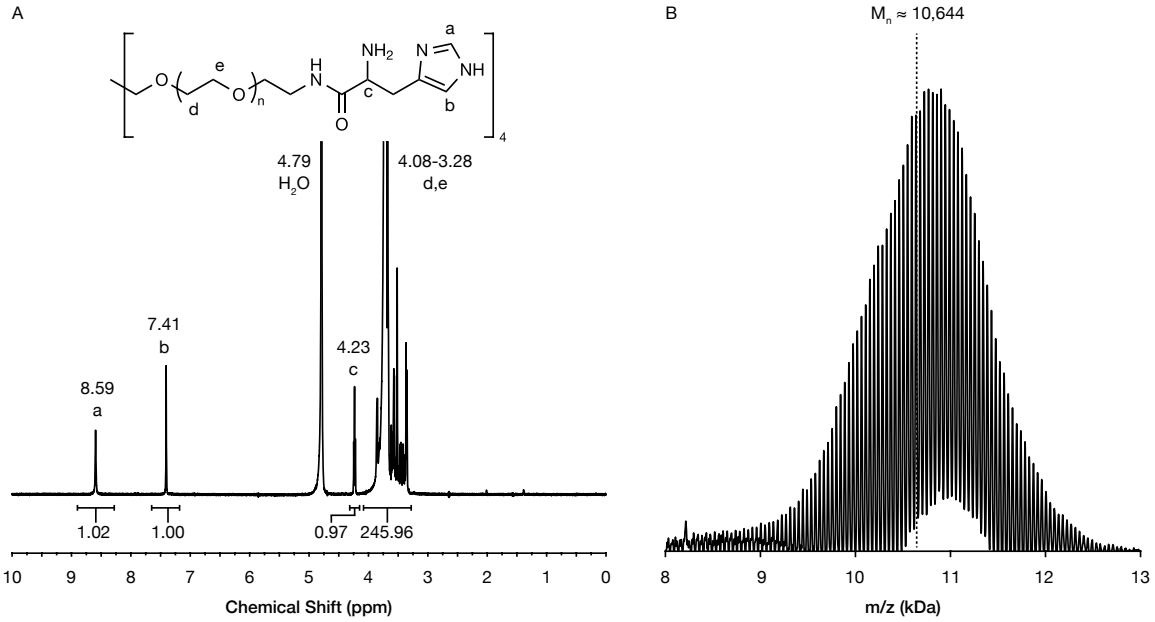

Figure S14: Characterization of the synthesized 4-arm poly (ethylene glycol) end functionalized with histidine. (*A*) ^{1}H-NMR of polymer in D_2O gives a coupling efficiency of 91.6 %. (*B*) MALDI-TOF results for the polymer give a number average molecular weight of 10 644 Da.